Investigation of Superconducting Gap Structure in HfIrSi using muon spin relaxation/rotation

A Bhattacharyya[1*], K Panda[1], D T Adroja[2,3], N Kase[4], P K Biswas[2], Surabhi Saha[5], Tanmoy Das[5†], M R Lees[6] and A D Hillier[2]

[1] Department of Physics, Ramakrishna Mission Vivekananda Educational and Research Institute, Howrah 711202, West Bengal, India
[2] ISIS Facility, Rutherford Appleton Laboratory, Chilton, Didcot Oxon, OX11 0QX, United Kingdom
[3] Highly Correlated Matter Research Group, Physics Department, University of Johannesburg, PO Box 524, Auckland Park 2006, South Africa
[4] Department of Applied Physics, Tokyo University of Science, Tokyo, 125-8585, Japan
[5] Department of Physics, Indian Institute of Science, Bangalore 560012, India
[6] Department of Physics, University of Warwick, Coventry CV4 7AL, United Kingdom

E-mail: *amitava.bhattacharyya@rkmvu.ac.in, †tnmydas@gmail.com

Abstract.
Appearance of strong spin-orbit coupling (SOC) is apparent in ternary equiatomic compounds with 5d-electrons due to the large atomic radii **no** of transition metals. SOC plays a major role in the emergence of unconventional superconductivity. Here we examined the superconducting state of HfIrSi using magnetization, specific heat, muon spin rotation/relaxation (μSR) measurements. Superconductivity is observed at $T_C = 3.6$ K as revealed by specific heat and magnetization measurements. From the transverse field μSR analysis it is clear that the temperature variation of superfluid density well fit by an isotropic BCS type s-wave gap structure. Additionally, we have calculated the superconducting carrier density $n_s = 6.6(1) \times 10^{26}$ m^{-3}, magnetic penetration depth $\lambda_L(0) = 259(2)$ nm and effective mass m$^* = 1.57(3)$ m$_e$ from TF-μSR data. The zero field μSR data of HfIrSi revealed absence of spontaneous magnetic moment below T_C, revealed the preserved time-reversal symmetry (TRS) in the superconducting state. Theoretical investigation suggests Hf and Ir atoms hybridize strongly along the c-axis of the lattice, which is responsible for the strong three-dimensionality of this system which screens the Coulomb interaction. As a result despite the presence of correlated d-electrons in this system, the correlation effect is weakened, promoting electron-phonon coupling to gain importance.

Keywords. Ternary equiatomic superconductor; Superconducting gap structure; Muon spin spectroscopy

PACS numbers: 71.20.Be, 74.70.Dd, 76.75.+i

1. Introduction

In recent years, ternary silicides and phosphides have drawn considerable attention due to their unusual superconducting properties [1, 2, 3, 4, 5, 6, 7, 8, 9, 10]. The discovery of superconductivity with transition temperatures ($T_{\rm C}$) more than 10 K in the 111-based transition metal phosphides [4] spurred research on similar compounds formed by replacing one or more elements in the material. As a result the isoelectronic system of arsenides MM'As and phosphides MM'P [where M = Zr or Hf and M' = Ru or Os], exhibits superconductivity at temperature as high as 12 K for hexagonal h-ZrRuAs [11], 13 K for h-ZrRuP [12] and 15.5 K for h-MoNiP [8]. Barz *et al.* [1] inferred a potentially enhanced density of states (DOS) at the Fermi level E_F due to reduced Ru-Ru bond length in h-ZrRuP with respect to pure Ru. Ternary compounds $TrT'X$ (Tr, T' = 4d or 3d transition elements and X is a group V or group IV atom) with a Fe_2P-type hexagonal structure [8]; the transition temperature, $T_{\rm C}$, of these 111-based compounds are pretty high, in some cases $T_{\rm C}$ is more than 10 K, for example, Shirotani *et al.* [10] reported superconducting transitions above 10 K for both h-ZrRuX (X = P, As or Si) and h-HfRuP. Some compounds of this 111-series with 4d and 5d electron exhibit $T_{\rm C}$ at more than 10 K for example, Shirotani *et al.* [10] reported superconducting transitions above 10 K for both h-ZrRuX (X = P, As or Si) and h-HfRuP. Either M and X atoms or Ru and X atoms occupy each layer of the hexagonal structure [9]. These atoms are located in each layer which are divided by a distance c and parallel to the $a-b$ plane. Shirotani *et al.* [9] reported the formation of the two-dimensional triangular clusters of Ru_3 in the $a-b$ plane.

111-based ternary compounds $TrT'X$ crystallizes in two type of layered structures: (a) the hexagonal Fe_2P-type (space group $P\bar{6}m2$), [6, 8, 4] and (b) the orthorhombic Co_2Si-type (space group $Pnma$) [7, 8, 4, 2]. At high temperatures and pressures orthorhombic phase modifies to higher-symmetry hexagonal structure. Amongst this group of superconductors, the Co_2P-type o-MoRuP has the highest $T_{\rm C}$ of 15.5 K [8]. Higher value of DOS at the Fermi level, which are ruled by the Mo-4d orbitals, are directly linked with the higher $T_{\rm C}$ in o-MoRuP [13]. Ching *et al.* [4] have estimated the DOS value for o-MoRuP is 0.46 states/eV atom. They have predicted that h-MoRuP may have a $T_{\rm C}$ above 20 K by assuming that the lattice dynamics and the electron-phonon coupling effect in o-ZrRuP, o-MoRuP, h-MoRuP, and h-ZrRuP crystals are reasonably close. Wong-Ng *et al.* [14] suggested that the main reasons for the distinction in $T_{\rm C}$ are the different values of DOS at the Fermi level. Recently, Kase *et al.* reported superconductivity in 5d transition metal compound o-HfIrSi with $T_{\rm C}$ 3.4 K [23]. As spin-orbit coupling (SOC) is directly proportional to Z^4, where Z is the atomic number, strong spin-orbit coupling must be important in o-HfIrSi [15] due to the high atomic numbers of Hf, Ir.

To shed the light upon the pairing mechanism in o-HfIrSi, we report a comprehensive study of o-HfIrSi using heat capacity, magnetization, zero and transverse field (ZF/TF) muon spin relaxation and rotation (μSR) measurements. Our recent μSR study on the caged type superconductors $R_5Rh_6Sn_{18}$ (R = Lu, Sc, and Y) [16, 17, 18] revealed that time-reversal symmetry (TRS) is broken due to strong spin-orbit coupling, while recently Singh *et. al.* [19] has reported that a system with strong spin-orbit coupling can break TRS. Our recent μSR study on the caged type superconductors $R_5Rh_6Sn_{18}$ (R = Lu, Sc, and Y) [16, 17, 18] revealed that time-reversal symmetry (TRS) is broken due to strong spin-orbit coupling. Furthermore, our ZF-μSR data does not reveal any evidence for spontaneous internal magnetic moment below $T_{\rm C}$, which indicates that for o-HfIrSi TRS is preserved. The temperature dependence of the superfluid density determined by means of TF$-\mu$SR support the conclusion that HfIrSi

is an s-wave BCS superconductor with only one isotropic energy gap, which is in accordance with the heat capacity results.

2. Experimental Details

Polycrystalline orthorhombic HfIrSi was prepared by melting stoichiometric quantities of high purity Hf, Ir, and Si in a water-cooled arc furnace. The as cast ingot was overturned and remelted several times to improve the phase homogeneity. The sample was annealed in a sealed quartz tube for 168 hrs at 1273 K. Powder X-ray diffraction data were collected using a conventional X-ray diffractometer. In order to ensure the $T_{\rm C}$ of the sample, we performed dc magnetic susceptibility measurements using a magnetic property measurement system (MPMS) in a temperature range of 1.5-10.0 K in an applied magnetic fields 10 Oe. Heat capacity measurements were performed down to 0.3 K using a physical property measurement system (PPMS)(Heliox-VL, Oxford Instruments).

To examine the superconducting pairing symmetry and microscopic properties of HfIrSi, we did the TF/ZF μSR experiments at the muon beamline of ISIS Pulsed Neutron and Muon Facility of the Rutherford Appleton Laboratory, United Kingdom using the MUSR spectrometer [20]. The high-quality powder of HfIrSi was mounted on a silver plate (99.995%) using GE low-temperature varnish and wrapped up with a silver film which was cooled down to 50 mK using a dilution refrigerator. To reduce the impact of the stray fields at the sample chamber the correction coils were used which assured the stray field to be within $\sim$ 0.001 Oe. 100% positive spin-polarized muons were implanted into the sample. The time dependence of the polarization of the implanted muons is given by $P_\mu(t) = G(t)P_\mu(0)$ where the function G(t) corresponds to the μ^+ spin autocorrelation function.A commonly measured quantity in μSR experiments is the time dependent asymmetry $A(t)$ which is proportional to $P_\mu(t)$. The asymmetry of the resulting positron was estimated using, $A(t) = [N_{\rm F}(t) - \alpha N_{\rm B}(t)]/[N_{\rm F}(t) + \alpha N_{\rm B}(t)]$, where $N_{\rm B}(t)$ and $N_{\rm F}(t)$ are the number of positrons counted in the backward and forward detectors respectively and α is a instrumental calibration constant determined in the normal state with a small (20 Oe) applied transverse magnetic field. ZF-μSR measurement is crucial to understand the type of pairing symmetry in superconductors [21]. Muon spin rotation and relaxation are very sensitive local probes which can be used to resolve the nature of the pairing symmetry in superconductors [21]. All the μSR data were analyzed using the WiMDA, a muon data analysis program [22]. The TF-μSR data were collected in the different temperatures between 0.05 K to 4 K in presence of 300 Oe ($> H_{\rm c1} = 10$ Oe) applied magnetic field, and ZF data were collected between 0.1 K and 4 K in absence of magnetic field.

3. Results and Discussion

3.1. Magnetization and Specific Heat

HfIrSi crystallizes in the orthorhombic structure with space group $Pnma$ (No. 62) [23, 15]. The lattice parameters are estimated to be $a = 6.523(5)$ Å, $b = 3.912(3)$ Å and $c = 7.353(4)$ Å from the powder X-ray diffraction study. The temperature (T) dependence of the magnetic susceptibility χ(T) of HfIrSi in an applied magnetic field of 10 Oe is shown in Fig. 1(a). $\chi(T)$ reveals a clear signature of superconductivity below the superconducting transition $T_{\rm C} = 3.6$ K. The magnetization isotherm $M(H)$ shown in Fig. 1(b) at 0.5 K is typical of

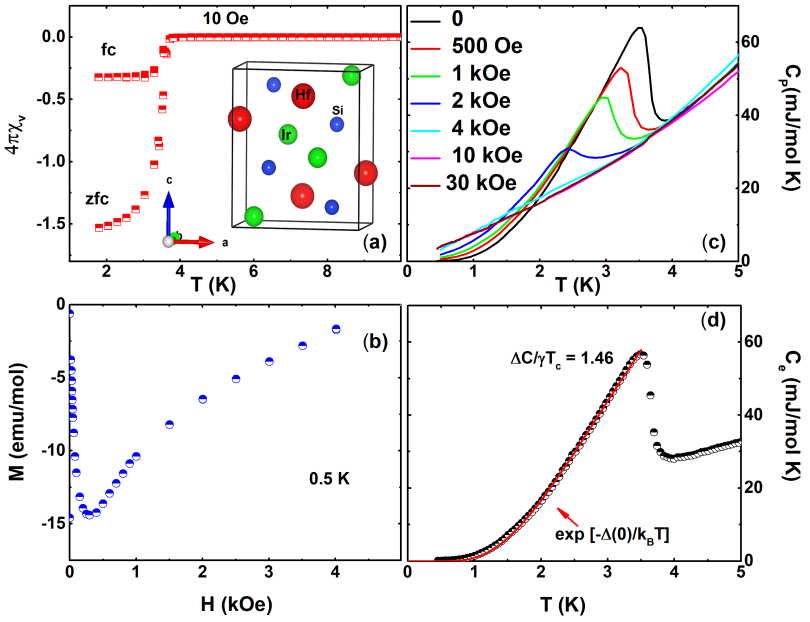

Figure 1. (a) The magnetic susceptibility $\chi(T)$ as a function of temperature collected in zero field cooled (ZF) and field cooled (FC) sequences under the applied field of 10 Oe . The inset shows a unit cell of orthorhombic crystal structure ($Pnma$) of HfIrSi. (b) Isothermal field dependence of magnetization at 0.5 K. (c) The temperature dependence of heat capacity $C_{\rm P}$ T for $0.45 \leq T \leq 5$ K measured in different applied magnetic fields. (d) Electronic contribution to zero field heat capacity data $C_{\rm e}$ as a function of temperature. The solid line indicates the fitting with the isotropic BCS expression.

type II superconductivity. The lower critical field was estimated from the $M-H$ curve at 0.5 K as 10 Oe. From the field dependence of the resistivity data [23] the upper critical field was estimated to be 22.3 kOe while the Pauli paramagnetic limit $18.4T_{\rm C} = 62.5$ kOe. Heat capacity ($C_{\rm P}$) as a function of temperature for $0.45 \leq T \leq 5$ K is shown in Fig. 1(c) at different applied magnetic fields. The normal state $C_{\rm P}$ was found to be independent of the external magnetic field. Above $T_{\rm C}$ in the normal state, $C_{\rm P}$ data described using $C_{\rm P}(T)/T = \gamma + \beta T^2$, where γ is the electronic heat capacity coefficient, and βT^3 βT^2 is the lattice contribution. Fitting gives $\gamma = 5.56(1)$ mJ mol $^{-1}$K^{-2} and $\beta = 0.17(2)$ mJ mol^{-1}K^{-4}. From the Debye model β is related to the Debye temperature $(\Theta_{\rm D}) = (\frac{12\pi^4}{5\beta} n N_{\rm A} R)^{1/3}$, where $R = 8.314$ J mol^{-1}K^{-1} is the gas constant and $n = 3$ is the number of atoms per formula unit in HfIrSi. From this relationship $\Theta_{\rm D}$ is estimated to be 323 K. The jump in the heat capacity $\Delta C_{\rm P}(T_{\rm C}) = 28.46(2)$ mJ/(mol-K) and $T_{\rm C} = 3.6$ K, yields $\Delta C/\gamma T_{\rm C} = 1.42(1)$ [23]. This value is close to 1.43 expected for the weak-coupling BCS superconductors [24].

Fig. 1(d) shows the temperature dependence of the electronic specific heat $C_{\rm e}$, obtained by subtracting the phonon contribution from $C_{\rm P}$. $C_{\rm e}$ used to investigate the superconducting gap symmetry. From the exponential dependence of $C_{\rm e}$ we obtained $\Delta(0) = 0.50(2)$ meV which is close to 0.51 meV, obtained from TF-μSR analysis. $\Delta(0) = 0.50(2)$ meV gives $2\Delta(0)/k_{\rm B}T_{\rm C} = 3.34(2)$, which is close to the value of 3.53 expected for weak-coupling BCS superconductors [25].

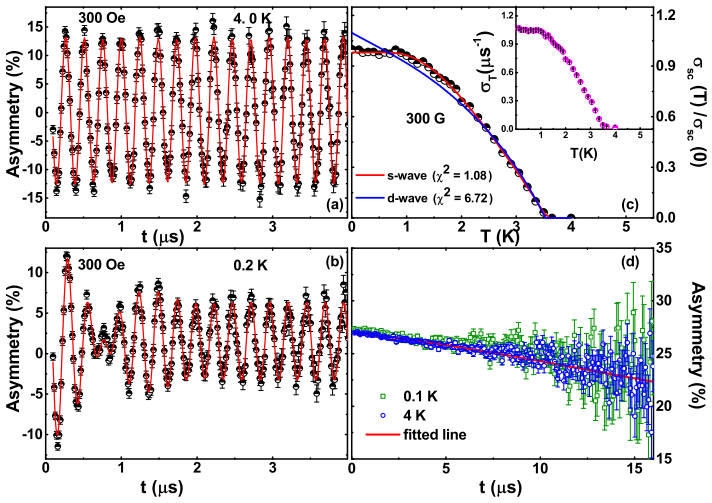

Figure 2. The time evolution of TF-μSR asymmetry spectra for HfIrSi recorded (a) at T = 4.0 K and (b) at T = 0.2 K in a magnetic field H = 300 Oe. The solid red line is the fit to the data using equation 1 as described in the text. (c) The temperature dependence of the superconducting depolarization rate $\sigma_{\rm sc}$(T) in presence of an applied magnetic field of 300 Oe. The inset shows the temperature variation of the total superconducting depolarization rate σ(T). (d) Zero field μSR time spectra for HfIrSi collected at 0.1 K (green square) and 4 K (blue circle) are shown together with lines that are least square fit to data.

3.2. TF-μSR analysis

To investigate the superconducting gap structure in *o*-HfIrSi, we have performed TF-μSR measurements. Figs. 2(a)-(b) display the TF-μSR asymmetry spectra taken at temperature above and below $T_{\rm C}$ in an applied magnetic field 300 Oe. Obviously, flux-line lattice [FLL] induced faster decay in the asymmetry spectra is observed below $T_{\rm C}$ [Figs. 2(b)] corresponds to the inhomogeneous field distribution of the superconducting state. The time evolution of the TF-μSR data at all temperatures above and below $T_{\rm C}$ is best described by a sinusoidal oscillatory function damped with a Gaussian relaxation and an oscillatory background term [26, 27, 28, 29]:

$$G_{\rm z1}(t) = A_1 \cos(\omega_1 t + \varphi) \exp(-\frac{\sigma^2 t^2}{2}) + A_2 \cos(\omega_2 t + \varphi) \tag{1}$$

Here A_1= 64.20% and A_2 = 35.80% are the initial asymmetries of the sample and the background which arises from the muons implanted directly into the silver sample holder that do not depolarize, ω_1 and ω_2 are the associated muon precision frequencies of the sample and the sample holder, respectively, φ is the initial phase of the offset and σ is the total muon spin relaxation rate. σ consists of two contribution: one is due to the inhomogeneous field variation across the superconducting vortex lattice ($\sigma_{\rm sc}$) and the other is is the normal state contribution ($\sigma_{\rm n}$ = 0.029 μs^{-1}) which is supposed to be fixed over the entire temperature range and was obtained from spectra measured above $T_{\rm C}$. σ is related to $\sigma_{\rm sc}$ and $\sigma_{\rm n}$ as $\sigma^2 = \sigma_{\rm sc}^2 + \sigma_{\rm n}^2$. Then subtracting the $\sigma_{\rm n}$ from σ, we obtain the superconducting contribution σ_{sc}. The temperature variation of the penetration depth/superfluid density modelled using [30, 31, 32, 33]

$$\frac{\sigma_{\rm sc}(T)}{\sigma_{\rm sc}(0)} = \frac{\lambda^{-2}(T, \Delta_{0,\rm i})}{\lambda^{-2}(0, \Delta_{0,\rm i})} \tag{2}$$

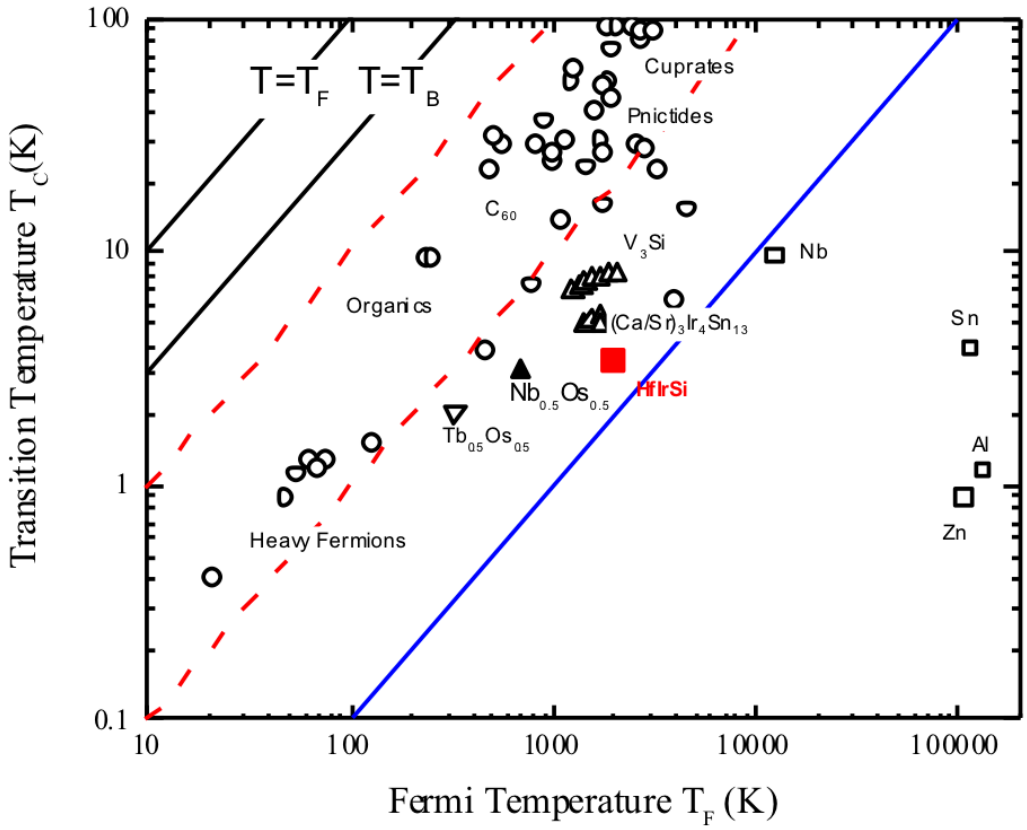

Figure 3. The superconducting transition temperature $T_{\rm C}$ vs the effective Fermi temperature $T_{\rm F}$, where HfIrSi is shown by solid red square. The solid black line correspond to the Bose-Einstein condensation temperature ($T_{\rm B}$). The unconventional superconductors fall within a common band for which $1/10 \geq (T_{\rm C}/T_{\rm F}) \geq 1/100$.

$$= 1 + \frac{1}{\pi}\int_0^{2\pi}\int_{\Delta({\rm T})}^{\infty}(\frac{\delta f}{\delta E}) \times \frac{EdEd\phi}{\sqrt{E^2 - \Delta(T,\Delta_i)^2}}$$

where $f = [1 + \exp(-E/k_{\rm B}T)]^{-1}$ is the Fermi function and $\Delta_{\rm i}(T,0) = \Delta_{0,{\rm i}}\delta(T/T_{\rm C}){\rm g}(\phi)$. $\Delta_{0,{\rm i}}$ is the value of superconducting gap. The temperature dependence of the superconducting gap is approximated by the relation $\delta(T/T_{\rm C}) = \tanh[1.82[1.018(T_{\rm C}/T-1)]^{0.51}]$ where ${\rm g}(\phi)$ refers to the angular dependence of the superconducting gap function. ${\rm g}(\phi)$ is replaced by (a) 1 for an s-wave gap, and (b) $|\cos(2\phi)|$ for a d-wave gap with line nodes [34, 35]. The data is best modeled using a single isotropic s-wave gap of 0.51(1) meV, which yield gap to $T_{\rm C}$ is $2\Delta/k_{\rm B}T_{\rm C} = 3.38(2)$, which is very close 3.34(2) obtained from the heat capacity data presented earlier, and indicating a weak-coupling superconductivity in HfIrSi. Furthermore, from TF-μSR result we have estimated the magnetic penetration depth $\lambda_{\rm L}(0) = 259(2)$ nm, superconducting carrier density $n_{\rm s} = 6.6(1) \times 10^{26}$ carriers m^{-3}, and the effective-mass enhancement $m^* = 1.57(3)m_{\rm e}$ respectively, for HfIrSi. Details calculation can be found on Ref. [36, 37, 38, 39, 40, 41]

3.3. ZF-μSR analysis

We have performed ZF-μSR measurement to check the appearance of spontaneous magnetic field in the ground state of HfIrSi. The time evolution of the zero field symmetry spectra above

and below and T_C (for T = 0.1 and 4.0 K) are shown in Fig. 2(d). The spectra are found to be identical. The ZF$-\mu$SR data well described using a damped Gaussian Kubo-Toyabe (KT) function and a background term, arises from muons that miss the sample and stop in the backing plate,

$$G_{z2}(t) = A_3 G_{KT}(t) e^{-\lambda_\mu t} + A_{bg}, \tag{3}$$

Here $G_{KT}(t)$ is the Gaussian Kubo-Toyabe function given by $G_{KT}(t) = [\frac{1}{3} + \frac{2}{3}(1 - \sigma_{KT}^2 t^2) \exp(-\frac{\sigma_{KT}^2 t^2}{2})]$. A_3 and A_{bg} is the asymmetry of the sample and background signal, respectively. σ_{KT} and λ_μ are the muon spin relaxation rates due to randomly oriented nuclear moments. The fitting parameters A_3, A_{bg} and σ_{KT} are independent of temperature. There is no significant change between the relaxation rates at 4.0 K ($\geq T_C$) and 0.1 K ($\leq T_C$). Fits to the ZF$-\mu$SR asymmetry data using Eq. 3 and shown by the solid lines in Fig. 2(d) give σ_{KT} = 0.06(1)5 μs^{-1} and λ_μ = 0.0046(3) μs^{-1} at 0.1 K and σ_{KT} = 0.06(2) μs^{-1} and λ_μ = 0.0046(1) μs^{-1} at 4 K. The values of both σ_{KT} and λ_μ at $T \leq T_C$ and $\geq T_C$ agree within error, indicating that TRS is preserved in the superconducting state of HfIrSi.

3.4. Uemura Classification Scheme

Here we have presented Uemura classification scheme [42, 43] which correlates the T_C and the effective Fermi temperature, T_F ($= \frac{\hbar^2 (3\pi^2)^{2/3} n_s^{2/3}}{2 k_B m^*}$). The value of n_s and m^* have been estimated from TF-μSR data. In this classification unconventional superconductors lie in between $1/10 \geq (T_C/T_F) \geq 1/100$. For conventional BCS superconductors $1/1000 \geq T_C/T_F$. The position of HfIrSi [$T_C/T_F = 3.6/2316.6 = 0.00155(4)$] on the plot places this material as being conventional superconductor.

3.5. Theoretical Investigations

HfIrSi belongs to the *Pnma*(62) space group and possess the orthorhombic crystal system with the *mmm* point group symmetry. We use Vienna Ab-initio Simulation Package (VASP) for density-functional theory (DFT) electronic structure calculations. The projected augmented wave (PAW) pseudo-potentials are used to describe the core electrons, and Perdew-Burke-Ernzerhof (PBE) functional is used for the exchange-correlation potential. Cut-off energy for plane wave basis set is used to be 500 eV. The Monkhorst-Pack k-mesh is set to $14 \times 14 \times 14$ in the Brillouin zone for the self-consistent calculation. We obtained the relaxed lattice parameters as $a = 3.944$ Å, $b = 6.499$ Å, $c = 7.376$ Å and $\alpha = \beta = \gamma = 90°$. To deal with the strong correlation effect of the d-electrons of the Ir atoms, we employed LDA+U method with $U = 2.8$ eV. For the Fermi surface and density of states calculations, we have used a larger k-mesh of $31 \times 31 \times 31$. We repeat the calculation with SOC and find no considerable change in the low-energy spectrum

Due to the involvement of the strongly correlated transition metals as well as possible SOC, one may anticipate superconductivity to be exotic in this material. However, the observation of conventional, time-reversal invariant superconductivity leads to an essential question: how does the phonon mediated attractive potential win over the strong Coulomb interaction to form conventional superconductivity.

To address this point, we investigate the DFT band structure as shown in Fig. 4. From the partial-DOS result in Fig. 4(a), we find that both transition metals Ir and Hf have nearly equal weight in the low-energy spectrum, and contribute mostly to the total DOS. Additionally, both transition metals have the corresponding 4*d* and 4*d* orbitals, respectively providing dominant

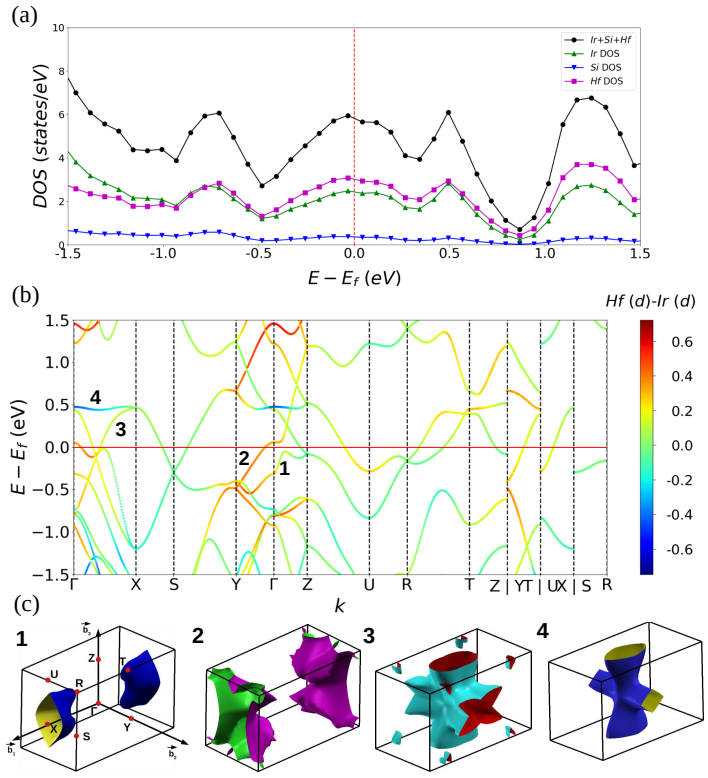

Figure 4. (a) Computed partial DOSs for the three atoms are compared along with the total DOS. We clearly observe that Hf and Ir atoms contribute dominantly to the low-energy spectrum. For both these atoms, 5d and 4d orbitals contribute mostly in this energy scale. (b) DFT result of band structure is plotted along the standard high-symmetric directions for the orthorhombic crystal structure of HfIrSi. The band structure is colored with a gradient colormap with blue color means Ir-d orbitals and red color means Hf-d orbitals. Four Fermi surfaces are denoted by '1', '2', '3', and '4' numbers. The result indicates that the bands near the Γ-point are dominated by Hf-d states while those near the 'Z' point gain more Ir-d weights. (c) Corresponding four Fermi surfaces in the 3D Brillouin zone. The color on the Fermi surface has no significance here.

contribution to the Fermi surfaces. The result indicates that these two atoms have strong hybridization in this system. This is confirmed by the visualization of the orbital weight distributions on the electronic structure as shown in Fig. 4(b). We plot here the difference in the orbital weights between the Ir-d and Hf-d orbitals. We indeed find that the bands near the Γ-point are dominated by the Hf-d orbitals while those on near the 'Z' (on the $k_z = \pm\pi$-plane) are contributed strongly by the Ir-d atoms. This result indicates that the Hf and Ir atoms hybridize rather strongly along the c-axis of the lattice. This hybridization is responsible for the strong three-dimensionality of this system which screens the Coulomb interaction. As a result despite the presence of correlated d electrons in this systems, the correlation effect is weakened, promoting electron-phonon coupling to gain importance.[54]

The Fermi surface topologies as shown in Fig. 4(c) confirm the strong three dimensionality in all four bands. Consistently we find two Fermi pockets near the Γ-points and two Fermi pockets centering the 'X'-points. The large Fermi surface volume is consistent with the large carrier density of this system as measured in our μSR experiments, and higher values of Fermi

temperature as presented in Fig. 3. These results are consistent with the weak correlation strength in this system.[55] Strong three-dimensionality can also reduce the relativistic effect and hence the SOC strength is reduced.

4. COMMENTS AND PERSPECTIVES

We have reported the magnetization, heat capacity, ZF and TF$-\mu$SR measurements in temperatures above and below $T_{\rm C}$ of HfIrSi, which crystallizes in the orthorhombic crystal structure. The heat-capacity and magnetization data confirmed bulk superconductivity in this material with $T_{\rm C} = 3.6$ K. We have estimated the temperature dependence of depolarization rate from the TF$-\mu$SR data in the field cooled mode associated with the vortex lattice. The temperature variation of $\sigma_{\rm sc}$ is better fit by an isotropic s-wave gap model than a d-wave model. The value of $2\Delta(0)/k_{\rm B}T_{\rm C} = 3.38$ obtained from the $s-$wave gap fit, suggests a weak-coupling BCS type superconductivity in HfIrSi. The ZF$-\mu$SR measurements reveal no sign of spontaneous field appearing below the $T_{\rm C}$ which suggests that the TRS is preserved in HfIrSi. Theoretical investigation suggests Hf and Ir atoms hybridize strongly along the c-axis of the lattice, which is responsible for the strong three-dimensionality of this system which screens the Coulomb interaction. As a result despite the presence of correlated d-electrons in this systems, the correlation effect is weakened, promoting electron-phonon coupling to gain importance. To date, a large number of equiatomic ternary metal compounds have been discovered with high superconducting transition temperatures and high critical magnetic fields, but μSR investigations have been carried out just on a few compounds. The present study will provide an invaluable comparison for the future μSR investigations on these families of compounds. The present results will help to develop a realistic theoretical model including the role of strong spin-orbital coupling to understand the origin of superconductivity in HfIrSi and also may help us to arrive at an empirical criterion for the occurrence of superconductivity with strong SOC and high T_c and H_{c2} in other equiatomic ternary systems.

Acknowledgments

AB would like to acknowledge the Department of Science and Technology (DST) India, for an Inspire Faculty Research Grant (DST/INSPIRE/04/2015/000169), and the UK-India Newton grant for funding support. KP acknowledge the financial support from DST India, for Inspire Fellowship (IF170620). DTA would like to thank the Royal Society of London for the UK-China Newton funding and the Japan Society for the Promotion of Science for an invitation fellowship. TD acknowledges the financial support from Science and Engineering Research Board (SERB), Department of Science & Technology (DST), Govt. of India for the Start Up Research Grant (Young Scientist).

References

[1] Barz H,Ku H C, Meisner G P, Fisk Z and Matthias B T 1980 *Proc. Natl. Acad. Sci.* **77**, 3132
[2] Müller R, Shelton R N, Richardson J W and Jacobson R A 1983 *J. Less-Common Met.* **42**, 177
[3] Seo D K, Ren J, Whangbo M H and Canadell E 1997 *Inorg. Chem.* **36**, 6058-6063
[4] Ching W Y, Xu Y N, Ouyang L, and Wong-Ng W 2003 *J. Appl. Phys.* **93**, 8209
[5] Keiber H, Wühl H, Meisner G P and Stewart G R 1984 *J. Low Temp. Phys.* **55**, 11
[6] Shirotani I, Takaya M,Kaneko I, Sekine C and Yagi T 2001 *Physica C* **357-360**, 329

[7] Shirotani I, Konno Y, Okada Y, Sekine C, Tado S and T. Yagi 1998 *Solid State Commun.* **108**, 967

[8] Shirotani I, Takeya M, Kaneko I, Sekine C and Yagi T 2000 *Solid State Comm.* **116**, 683

[9] Shirotani I, Tachi K, Konnon Y, Todo S and Yagi T 1999 *Phil. Mag. Part B* **79:5**, 767-776

[10] Shirotani I, Tachi K, Takeda K, Todo S, Yagi T and Kanoda K 1995 *Phys. Rev. B* **52**, 6197

[11] Meisner G P, Ku H C and Barz H 1983 *Matter. Res. Bull.* **18**, 983

[12] Shirotani I, Ichihashi N, Nozawa K, Kinoshita M, Yagi T, Suzuki K and Enoki T 1993 *Jpn. J. Appl. Phys.* **32-3**, 695

[13] Kita T and Arai M 2004 *Phys. Rev. B* **70**, 224522

[14] Wong-Ng W, Ching W Y, Xu Y N, Kaduk J A, Shirotani I and Swartzendruber L 2003 *Phys. Rev. B* **67**, 144523

[15] Wang X-Z, Chevalier B, Etourneau J and Hagenmuller P 1985 *Mater. Res. Bull.* **20**, 517

[16] Bhattacharyya A, Adroja D T, Quintanilla J, Hillier A D, Kase N, Strydom A M and Akimitsu J 2015 *Phys. Rev. B* **91**, 060503

[17] Bhattacharyya A, Adroja D T, Kase N, Hillier A D, Akimitsu J and Strydom A M 2015 *Sci. Rep.* **5**, 12926

[18] Bhattacharyya A, Adroja D T, Kase N, Hillier A D, Strydom A M and Akimitsu J 2018 *Phys. Rev. B* **98**, 024511

[19] Singh R P, Hillier A D, Mazidian B, Quintanilla J, Annet J F, Paul D M, Balakrishnan G and Lees M R 2014 *Phys. Rev. Lett.* 112, 107002

[20] Lee S L,Kilcoyne S H and Cywinski R 1999 *Muon Science: Muons in Physics, Chemistry and Materials* (SUSSP and IOP, Bristol, UK).

[21] Sonier J E, Brewer J H and Kiefl R F 2000 *Rev. Mod. Phys.* **72**, 769

[22] Pratt F L 2000 *Physica B* **289-290**, 710

[23] Kase N, Suzuki H, Nakano T and Takeda N 2016 Supercond. Sci. Technol **29**, 035011

[24] Tinkham M 1975 *Introduction to Superconductivity* McGraw-Hill, New York

[25] Bardeen J, Cooper L N and J. R. Schrieffer 1957 *Phys. Rev.* **106**, 162

[26] Bhattacharyya A, Adroja D T, Smidman M and Anand V K 2018 *Sci. China-Phys. Mech. Astron.* **61**, 127402

[27] Adroja D T, Bhattacharyya A, Biswas P K, Smidmann M, Hillier A D, Mao H, Luo H, Cao G H, Wang Z and Wang C 2017 *Phys. Rev. B* **96**, 144502

[28] Bhattacharyya A, Adroja D T, Panda K, Saha S, Das T, Machado A J S, Grant T W, Fisk Z, Hillier A D and Manfrinetti P 2019 *Phys. Rev. Lett.* **122**, 147001

[29] Anand V K, Britz D, Bhattacharyya A, Adroja D T, Hillier A D, Strydom A M, Kockelmann W, Rainford B D and McEwen K A 2014 *Phys. Rev. B* **90 (1)**, 014513

[30] Prozorov R and Giannetta R W 2006 *Supercond. Sci. Technol.* **19**, R41

[31] Adroja D T, Bhattacharyya A, Telling M, Feng Y, Smidman M, Pan B, Zhao J, Hillier A D, Pratt F L and Strydom A M 2015 *Phys. Rev. B* **92**, 134505

[32] Adroja D T, Bhattacharyya A, Smidman M, Hillier A D, Feng Y, Pan B, Zhao J, Lees M R, Strydom A M and Biswas P K 2017 *J. Phys. Soc. Jpn.* **86**, 03470

[33] Bhattacharyya A, Adroja D T, Hillier A D, Jha R, Awana V P S, Strydom A M 2017 *J. Phys: Cond. Matt.* **29**, 265602

[34] Pang G, Smidman M, Jiang W, Bao J, Weng Z, Wang Y, Jiao L, Zhang J, Cao G and Yuan H 2015 *Phys. Rev. B* **91**, 220502

[35] Annett J F 1989 *Adv. Phys.* **39**, 83-126

[36] Brandt E H 2003 *Phys. Rev. B* **68**, 054506

[37] Chia E E, Salamon M, Sugawara H and Sato H 2004 *Phys. Rev. B* **69**, 180509

[38] Amato A 1997 *Rev. Mod. Phys.* **69**, 1119

[39] McMillan W L 1968 *Phys. Rev.* **167**, 331

[40] Bhattacharyya A, Adroja D T, Biswas P K, Sato Y J, Lees M R, Aoki D and Hillier A D arXiv: 1901.04796.

[41] Das D, Gupta R, Bhattacharyya A, Biswas P K, Adroja D T and Hossain Z 2018 *Phys. Rev. B* **97**, 184509
[42] Uemura Y J, Luke G M, Sternlieb B J, Brewer J H, Carolan J F, Hardy W N, Kadono R, Kempton J R, Kiefl R F, Kreitzman S R, Mulhern P, Riseman T M, Williams D Ll, Yang B X, Uchida S, Takagi H, Gopalakrishnan J, Sleight A W, Subramanian M A, Chien C L, Cieplak M Z, Xiao G., Lee V Y, Statt B W, Stronach C E, Kossler W J and Yu X H 1989 *Phys. Rev. Lett.* **62**, 2317
[43] Hillier A D and Cywinski R 1997 *Appl. Mag. Reson.* **13**, 95
[44] Perdew J P, Burke K. and Matthias E 1996 *Phys. Rev. Lett.* **77**, 18
[45] Blöchl P. E. 1994 *Phys. Rev. B* **50**, 24
[46] Hicks D, Oses C, Gossett E, Gomez G, Taylor R H, Toher C, Mehl M J, Levy O and Curtarolo S. 2018 *Acta Cryst.* **A74**, 184-203.
[47] Ong S P, Richards W D, Jain A, Hautier G, Kocher M, Cholia S, Gunter D, Chevrier V L, Persson K A and Ceder G 2013 *Computational Materials Science* **68**, 0927-0256
[48] Liechtenstein A I, Anisimov V I and Zaanen J 1995 *Phys. Rev. B* **52**, 8
[49] Dudarev S L, Botton G A, Savrasov S Y, Humphreys C J and Sutton A P 1998 *Phys. Rev. B* **57**, 3
[50] G. Kresse and J. Hafner 1993 *Phys. Rev. B* **47**, 558
[51] Kresse G and Hafner J 1994 *Phys. Rev. B* **49**, 14251
[52] Kresse G and Furthmüller J 1996 *Comput. Mat. Sci.* **6** 15
[53] Kresse G and Furthmüller J 1996 *Phys. Rev. B* **54**, 11169
[54] Das T and Dolui K 2015 *Phys. Rev. B* **91**, 094510; Yin Z P, Kutepov A and Kotliar G 2013 *Phys. Rev. X* **3**, 021011
[55] Das T, Markiewicz R S and Bansil A 2014 *Adv. Phys.* **63**, 151-266